Journal of the American Heart Association

ORIGINAL RESEARCH

Impaired Cardiac Sympathetic Activity Is Associated With Myocardial Remodeling and Established Biomarkers of Heart Failure

Luis M. da Silva, PhD; Andréa Coy-Canguçu, MD; Layde R. Paim, PhD; Adriana A. Bau, MD; Camila Nicolela Geraldo Martins, MD; Stephan Pinheiro, MD; Vinicius Citeli Ribeiro, MD; Walter E. Magalhães Rocha, MD, PhD; Jose R. Mattos-Souza, MD, PhD; Roberto Schreiber, PhD; Lígia Antunes-Correa, PhD; Andrei Sposito, MD, PhD; Wilson Nadruz Jr, MD, PhD; Celso D. Ramos, MD, PhD; Tomas Neilan, MD; Michael Jerosch-Herold, PhD; Otávio R. Coelho-Filho, MD, PhD, MPH

BACKGROUND: ^{123}Iodine-meta-iodobenzylguanidine scintigraphy is useful for assessing cardiac autonomic dysfunction and predict outcomes in heart failure (HF). The relationship of cardiac sympathetic function with myocardial remodeling and diffuse fibrosis remains largely unknown. We aimed to evaluate the cardiac sympathetic function of patients with HF and its relation with myocardial remodeling and exercise capacity.

METHODS AND RESULTS: Prospectively enrolled patients with HF (New York Heart Association class II–III) were stratified into HF with preserved left ventricular ejection fraction [LVEF] ≥45%) and reduced LVEF. Ventricular morphology/function and myocardial extracellular volume (ECV) fraction were quantified by cardiovascular magnetic resonance, global longitudinal strain by echocardiography, cardiac sympathetic function by heart-to-mediastinum ratio from ^{123}iodine-meta-iodobenzylguanidine scintigraphy. All participants underwent cardiopulmonary exercise testing. The cohort included 33 patients with HF with preserved LVEF (LVEF, 60±10%; NT-proBNP [N-terminal pro-B-type natriuretic peptide], 248 [interquartile range, 79–574] pg/dL), 28 with HF with reduced LVEF (LVEF, 30±9%; NT-proBNP, 743 [interquartile range, 250–2054] pg/dL) and 20 controls (LVEF, 65±5%; NT-proBNP, 40 [interquartile range, 19–50] pg/dL). Delayed (4 hours) ^{123}iodine-meta-iodobenzylguanidine heart-to-mediastinum ratio was lower in HF with preserved LVEF (1.59±0.25) and HF with reduced LVEF (1.45±0.16) versus controls (1.92±0.24; P<0.001), and correlated negatively with diffuse fibrosis assessed by ECV (R=−0.34, P<0.01). ECV in segments without LGE was increased in HF with preserved ejection fraction (0.32±0.05%) and HF with reduced left ventricular ejection fraction (0.31±0.04%) versus controls (0.28±0.04, P<0.05) and was associated with the age- and sex-adjusted maximum oxygen consumption (peak oxygen consumption); (R=−0.41, P<0.01). Preliminary analysis indicates that cardiac sympathetic function might potentially act as a mediator in the association between ECV and NT-proBNP levels.

CONCLUSIONS: Abnormally low cardiac sympathetic function in patients with HF with reduced and preserved LVEF is associated with extracellular volume expansion and decreased cardiopulmonary functional capacity.

Key Words: cardiac magnetic resonance ■ cardiac sympathetic function ■ heart failure ■ interstitial fibrosis

Heart failure (HF) is a growing health care challenge with high morbidity and mortality rates.[1,2] It is estimated that 21 in 1000 individuals aged ≥65 are affected by HF, corresponding to ≈6.2 million American adults.[3] This public health burden is compounded by the limited advancements in the management of HF

Correspondence to: Otávio R. Coelho-Filho, MD, PhD, MPH, Discipline of Cardiology, Department of Internal Medicine, Hospital das Clínicas, University of Campinas, UNICAMP, Rua Vital Brasil, 251-Cidade Universitária "Zeferino Vaz," Campinas, SP 13083-888, Brazil. Email: orcfilho@unicamp.br

This manuscript was sent to Erik B. Schelbert, MD, MS, Associate Editor, for review by expert referees, editorial decision, and final disposition.

Supplemental Material is available at https://www.ahajournals.org/doi/suppl/10.1161/JAHA.124.035264

For Sources of Funding and Disclosures, see page 12.

JAHA is available at: www.ahajournals.org/journal/jaha

CLINICAL PERSPECTIVE

What Is New?

- Patients with heart failure (HF) with reduced ejection fraction and preserved ejection fraction exhibited abnormal cardiac sympathetic function characterized by a lower heart-to-mediastinum ratio on delayed (4 hours) ^{123}iodine-meta-iodobenzylguanidine scintigraphy images compared with controls.
- Sympathetic function, evaluated through ^{123}iodine-meta-iodobenzylguanidine single-photon emission computed tomography, was significantly associated with several markers of myocardial remodeling and left ventricular dysfunction, including left ventricular mass index (R=−0.48) and left ventricular cardiomyocyte mass index (R=−0.46), left ventricular end-diastolic volume index (R=−0.44), global longitudinal strain (R=−0.54), and left ventricular ejection fraction (R=0.41).
- Myocardial fibrosis, a hallmark of HF pathology is negatively associated with reduced sympathetic function, indicating that diffuse myocardial fibrosis may reduce sympathetic nerve density.

What Are the Clinical Implications?

- The inverse correlation observed between extracellular volume and ^{123}iodine-meta-iodobenzylguanidine heart-to-mediastinum ratio indicates that the build-up of diffuse interstitial fibrosis and extracellular matrix expansion reduces sympathetic innervation density in HF.
- Additional investigations are necessary to delve into the wider mechanistic and therapeutic ramifications of sympathetic function in patients with HF with preserved ejection fraction and HF with reduced ejection fraction.

Nonstandard Abbreviations and Acronyms

ADMIRE-HF	AdreView Myocardial Imaging for Risk Evaluation in Heart Failure
^{123}I-MIBG	^{123}iodine-meta-iodobenzylguanidine
ECV	extracellular volume
GLS	global longitudinal strain
HFpEF	heart failure with preserved ejection fraction
HFrEF	heart failure with reduced ejection fraction
H/M	heart-to-mediastinum
LGE	late gadolinium enhancement
Vo_2	oxygen consumption

with preserved ejection fraction (HFpEF). Measurement of NT-proBNP (N-terminal pro-B-type natriuretic peptide) and cardiopulmonary exercise capacity play a pivotal role in many clinical guidelines for the diagnosis of HF.[4,5] These important clinical tests provide prognostically predictive measures of the impact of HF, but therapeutic advances may require a better mechanistic understanding of the relation between myocardial pathophysiology and clinical markers of HF.

Derangement of cardiac sympathetic function is a distinct characteristic of the clinical syndrome of HF. Myocardial scintigraphy with ^{123}iodine-meta-iodobenzylguanidine (^{123}I-MIBG) could play an important role as a prognostic tool in the evaluation of cardiac sympathetic dysfunction in HF. The heart-to-mediastinum (H/M) ratio from delayed (≈4 hours after injection) ^{123}I-MIBG images is a predictor of sudden death and cardiac events in patients with HF.[6,7] There remain important gaps in our understanding of how myocardial sympathetic function is related to myocardial tissue remodeling in patients with HF, and to standard clinical measures of HF severity like cardiopulmonary exercise capacity.

Cardiac magnetic resonance (CMR) imaging, and specifically mapping of the T1 relaxation in the myocardium, can provide important insights on adverse tissue remodeling, such as the expansion of the extracellular volume (ECV). ECV has been evaluated as a biomarker of *diffuse* tissue fibrosis in HF and was associated with adverse outcomes, including hospitalization for HF and death.[8] We hypothesized that the expansion of the ECV may be associated with reduced sympathetic function because of lower sympathetic nerve density. Whether diffuse fibrosis and reduced myocardial sympathetic activity are independent predictors of cardiopulmonary exercise capacity and HF severity also remains largely unknown.

The aim of the current study was to evaluate cardiac sympathetic activity through ^{123}I-MIBG scintigraphy in patients with both HFrEF and HFpEF, to analyze its association with ECV expansion, and to determine the effects of ECV and cardiac sympathetic activity on NT-proBNP and cardiopulmonary exercise capacity.

METHODS

The data underlying this article will be shared on reasonable request to the corresponding author.

Study Participants

Patients with HF were required to be aged ≥18 years, present functional limitations due to HF symptoms (New York Heart Association class ≥II) according to the established Framingham criteria,[9] as well as the recently published universal definition for HF,[10]

be euvolemic under optimized treatment for HF, and have a previous transthoracic echocardiogram report confirming structural abnormalities or systolic dysfunction. Patients with HF with claustrophobia, pacemaker, Chagas disease, recent acute coronary syndrome (within 6 months), hypertrophic cardiomyopathy, infiltrative heart disease, significant valvular disease, or any impediment to exercise were excluded. Additionally, patients with documented or suspected hereditary cardiomyopathies, hemochromatosis, and cardiac amyloidosis were excluded. Upon enrollment, patients underwent echocardiography, which was then employed to classify patients as having either HFrEF (left ventricular ejection fraction [LVEF] <45%) or HFpEF (LVEF ≥45%). The H_2FPEF(heavy, hypertensive, atrial fibrillation, pulmonary hypertension, elder, filling pressure) score, a validated instrument for the assessment of patients with HFpEF, was used to corroborate the diagnosis of HFpEF.[11]

Patients with HF and healthy controls underwent ^{123}I-MIBG, CMR, echocardiography, laboratory testing, serum biomarker assessment, and cardiopulmonary exercise testing within 45 days of enrollment, from February 2017 until April 2019 (Figure 1). All procedures were conducted in a blinded manner with respect to clinical information or subject groups (control, HFrEF, or HFpEF). This study was performed in line with the principles of the Declaration of Helsinki. All participants provided written informed consent, and approval was granted by the Ethics Committee of the State University of Campinas (CAAE 63097016.5.2011.54.04).

Echocardiography

Two-dimensional echocardiographic evaluation (Vivid-S70, GE Healthcare, Milwaukee, WI) using a 3.5-MHz transducer was carried out with patients placed in the left lateral decubitus position, as recommended by current guidelines of the American Society of Echocardiography.[12] The E/A ratio was obtained with pulsed Doppler by averaging values from 3 consecutive cardiac cycles in 3 different alignments at closure of the mitral valve leaflets, with an acoustic window in the 4-chamber apical axis. To obtain systolic strain index, diastolic strain index, and mean longitudinal strain (%), 2-dimensional analysis of myocardial strain was performed by acquiring basal, medium, and apical axial images in short axis and 4- and 2-chamber views.

^{123}Iodine-Meta-Iodobenzylguanidine

To assess cardiac sympathetic autonomic nervous system function, planar imaging and single-photon emission computed tomography/computed tomography) were performed using a 2-channel single-photon emission computed tomography/computed tomography scanner (Symbia T, Siemens, Erlangen, Germany). For thyroid protection, patients received 10 mL of potassium iodide syrup (corresponding to 200 mg) 30 minutes before the injection of ^{123}I-MIBG and were encouraged to drink large volumes of fluids in the 48 hours following the exam for excretion of the radiopharmaceutical. ^{123}I-MIBG, diluted with saline, was slowly infused through a peripheral vein over 1 to 2 minutes, totaling 5 mCi to 10 mCi of ^{123}I-MIBG in 5 mL of solution. Planar and single-photon emission computed tomography /single-photon emission computed tomography imaging was performed at 15 minutes (“early”) and 4 hours (“delayed”) following the injection of ^{123}I-MIBG, with the patient in supine position with arms raised above the head. To obtain anterior planar images of the thorax, a low-energy, high-resolution collimator was positioned as closely as possible to the heart. Images were acquired for 10 minutes in the anterior view and stored in a 256×256 matrix for 2500 kcounts (10 minutes). Detectors were kept in a 90° configuration, and the images, acquired over 30 seconds per projection, were stored in a matrix of 128×128.[13] The ^{123}I-MIBG, early (at 15 minutes), and delayed (at 4 hours) H/M ratios, as well as the washout rate, were obtained following established protocols.[13] All ^{123}I-MIBG data were analyzed blinded to any clinical information, using a dedicated post-processing software (SyngoVia, Siemens, Erlangen, Germany).

Cardiac Magnetic Resonance Imaging

CMR imaging was performed with a 3-Tesla system (Achieva, Philips Medical Systems, Best, The Netherlands), with the patient in the supine position, and using a 6-element phased-array surface coil. ECG-triggered cine imaging with steady-state free precession was used to assess cardiac morphology and function from short- and long-axis views for field of view, 300 mm; echo time, 1.5 ms; repetition time, 3 ms; flip angle, 50°; 256×196 matrix; 8-mm slice, and in-plane spatial resolution, 1.5 mm. Late gadolinium enhancement (LGE) images were obtained at ≈10 minutes after a cumulative gadolinium dose of 0.2 mmol/kg (Gadoterate-meglumine; Dotarem, Guerbet, Aulnay-sous-Bois, France) using a segmented, phase-sensitive inversion recovery–prepared gradient-echo acquisition, triggered every other heartbeat. LGE was quantified in the phase-sensitive inversion recovery–prepared images as percentage of total left ventricular (LV) mass using a 5SD criterion. T2 mapping was acquired before contrast administration in a single short-axis slice using a multiecho gradient-spin-echo sequence as previously described.[14] T1 mapping was performed using a Modified Look-Locker Imaging

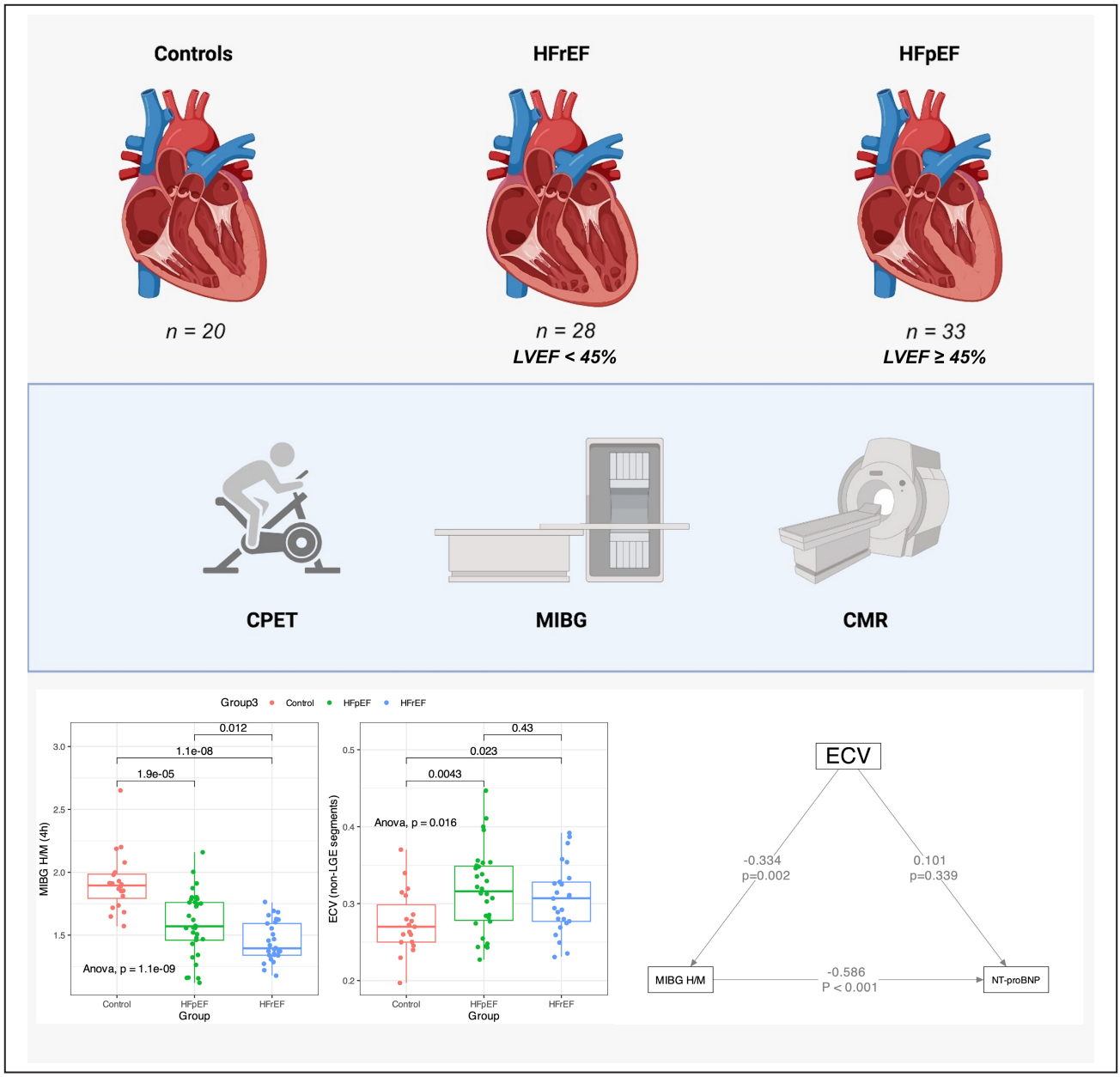

Figure 1. Study overview.
Patients with HF stratified by LVEF and controls underwent CMR, cardiopulmonary exercise testing (CPET), and cardiac ^{123}I-MIBG scintigraphy. While ^{123}I-MIBG H/M was significantly lower among HF individuals, ECV—a marker of interstitial fibrosis—was elevated and demonstrated an indirect effect mediated by the myocardial ^{123}I-MIBG H/M on NT-proBNP. CMR indicates cardiac magnetic resonance; ECV, expanded extracellular volume; HF, heart failure; HFpEF, heart failure with preserved ejection fraction; HFrEF, heart failure with reduced ejection fraction; H/M, heart-to-mediastinum; ^{123}I-MIBG, ^{123}iodine-meta-iodobenzylguanidine; and LVEF, left ventricular ejection fraction.

sequence before and 4 times after contrast administration,[15] using a 5s(3s)3s Modified Look-Locker imaging acquisition scheme for native T1, and 4s(1s)3s(1s)2s for postcontrast T1. The postcontrast acquisitions were conducted at intervals of 10 minutes after contrast administration, starting 5 minutes after its introduction, for ECV quantification, asperously described.[16,17] ECV was estimated by linear regression of myocardial R1 against blood R1 and using the blood hematocrit of a blood sample drawn at the time of CMR. Both a global LV average of ECV and an average using only LV segments without LGE were calculated for each patient. Unless stated otherwise, ECV in this article refers to the LV average with exclusion of segments with LGE. LV cardiomyocyte mass was estimated as the product of (1–ECV) and total LV mass, respectively. The MASS CMR software (Mass Research, Leiden University Medical Center, Leiden, Netherlands) was used for

all CMR image analysis, which was conducted in a blinded fashion to any clinical data.

Cardiopulmonary Exercise Testing

Cardiopulmonary exercise testing was performed using interface analysis of respiratory gases through an ergo spirometer (MedGraphics, St. Paul, MN). A maximum ramp protocol was performed with an increase of 5 to 15 W/min in workload until exhaustion. Oxygen consumption (V_{O_2}), carbon dioxide production, and respiratory exchange ratio were calculated using the breath-to-breath technique. Peak V_{O_2} was defined as the highest consumption of O_2, obtained by averaging data from the last 30 seconds of peak effort.[18] A resting 12-lead ECG was recorded using standard techniques immediately before the initiation of the cardiopulmonary exercise testing.

Blood Sampling and Measurement of Biomarkers

Blood samples were obtained after 12-hour fasting for the following laboratory parameters and biomarkers: hematocrit, renal function, lipid profile, glucose, glycosylated hemoglobin, C-reactive protein, high-sensitivity cardiac troponin T (hs-cTnT), and NT-proBNP. These laboratory tests followed standard techniques performed with commercially available kits (Roche Diagnostics, Germany).

Statistical Analysis

Results are presented as mean and SD or error (SE), or median with interquartile range (IQR) if not normally distributed. Variables were compared using the Mann–Whitney *U* testing or *t* tests. Continuous variables were compared between groups (HFrEF, HFpEF, and controls) by pairwise *t* tests or Wilcoxon signed-rank tests, with adjustment of *P* values for multiple testing by Holm's method. Statistical significance was defined as $P \leq 0.05$. Correlations were assessed using Pearson's method. Mediation analysis was used to determine the direct effect of ECV on NT-proBNP, and its indirect effect mediated by sympathetic innervation assessed by the ^{123}I-MIBG H/M ratio. Mediation analysis was performed with the "lavaan" package (https://cran.r-project.org/web/packages/lavaan/index.html) for structural equation modeling, and confidence intervals for the model coefficients were generated by the bootstrap method. The residual root mean square error of approximation, a fit statistic of the average of standardized residuals between the observed and the hypothesized covariance, was used to assess fit quality. A root mean square error of approximation value <0.05 is considered to indicate good convergence of the fit to the data. Principal component analysis was used to identify the main characteristics of HFrEF and HFpEF phenotypes, other than LVEF through the following variables: NT-proBNP (log-transformed), hs-cTnT (log-transformed), LV LGE, QRS duration, the diastolic function index E/e′ from echocardiography, mean LV ECV for all segments without LGE, delayed ^{123}I-MIBG H/M ratio, and LV mass-to-end-diastolic-volume ratio. Statistical analysis was performed with the R program version 4.3.2 (R Foundation for Statistical Computing, Vienna, Austria; URL: https://www.R-project.org/).

RESULTS

Clinical Characteristics and Serum Biomarkers

Sixty-one patients with symptomatic HF (33 with HFpEF, 28 with HFrEF) were recruited from the HF outpatient clinic of a tertiary university hospital (Hospital Clinics of the University of Campinas, Campinas, São Paulo, Brazil), as well as 20 healthy controls. Their demographic and clinical characteristics are listed in Table 1. All enrolled patients with HF were symptomatic, though following guidelines for medical therapy in HF and regular patient follow-up. Notably, a majority of HFpEF patients were classified as New York Heart Association functional class III (57.6%), while the predominant New York Heart Association class for patients with HFrEF was class II (60.8%; Table 1). In terms of pathogenesis, no significant differences were observed within HF phenotypes, as evidenced by a comparable proportion of individuals presenting with ischemic and nonischemic pathogenesis among the recruited groups (Table 1). The mean H_2FPEF score among patients with HFpEF was equal to 4.5 (1–8).

Patients with HFpEF were older (HFpEF, 62 [IQR, 50–70]; HFrEF, 53 [IQR, 47–62]; controls, 41 [IQR, 31–52] years, control versus HFpEF or HFpEF; $P<0.01$; Table 1). Both HF groups had comorbidities, such as hypertension, diabetes, and dyslipidemia, but the prevalence of diabetes (69%) and hypertension (91%) were higher in the HFpEF group. Patients with HFrEF were undergoing guideline-recommended pharmacotherapy characterized by 100% use of angiotensin receptor–neprilysin inhibitor, angiotensin-converting enzyme inhibitors, or angiotensin receptor blockers, β blockers, and diuretics, and 68% use of aldosterone antagonists (Table 1). In contrast, patients diagnosed with HFpEF were predominantly receiving diuretics (75%) to manage hypervolemia/congestion and medications to directly control comorbidities such as hypertension, diabetes, and dyslipidemia (Table 1).

HFrEF patients had higher levels of NT-proBNP compared with both patients with HFpEF and controls (HFpEF, 248 [IQR, 79–574], HFrEF, 743 [IQR,

Table 1. Patient Demographic and Clinical Characteristics

Variables	Summary statistics			*P* values (Holm adj.)		
	Control N=20*	HFpEF N=33*	HFrEF N=28*	Control vs HFpEF	Control vs HFrEF	HFpEF vs HFrEF
Female, n (%)	12 (60)	18 (55)	16 (57)	1.00	1.00	1.00
Age, y	41 (31–52)	62 (50–70)	53 (47–62)	<0.01	<0.01	0.05
Height, cm	165 (8)	162 (8)	163 (8)	0.25	0.40	0.24
Weight, kg	66 (10)	82 (15)	80 (12)	<0.01	<0.01	0.56
Body surface area	1.73 (0.15)	1.87 (0.18)	1.86 (0.14)	<0.01	0.013	0.78
Body mass index, kg/m^2	24.1 (3.3)	31.2 (5.9)	30.2 (5.2)	<0.01	<0.01	0.49
Hemodynamic data						
Resting heart rate, bpm	80 (12)	70 (12)	80 (14)	0.01	0.27	0.01
Systolic blood pressure, mm Hg	110 (19)	140 (17)	130 (23)	<0.01	0.15	<0.01
Diastolic blood pressure, mm Hg	80 (8)	90 (11)	80 (12)	<0.01	0.34	<0.01
NYHA functional class						
Class II	0 (0)	14 (42.4)	17 (60.8)			
Class III	0 (0)	19 (57.6)	11 (39.2)			
Comorbidities						
Hypertension	0 (0)	29 (91)	21 (75)	<0.01	<0.01	0.20
Diabetes	0 (0)	22 (69)	12 (43)	<0.01	<0.01	0.08
Dyslipidemia	0 (0)	24 (75)	21 (75)	<0.01	<0.01	0.9
Smoking	0 (0)	8 (25)	7 (25)	0.07	0.07	1.00
History of myocardial infarction	0 (0)	3 (9)	4 (14)	0.47	0.50	0.31
History of atrial fibrillation (permanent or paroxysmal)	0 (0)	10 (30)	3 (11)	0.05	0.36	0.18
History of prior revascularization (PCI or CABG)	0 (0)	6 (18.2)	2 (7.1)	0.34	0.63	0.56
Heart failure pathogenesis						
Ischemic	0 (0)	10 (31)	9 (32)	<0.01	0.16	0.06
Not ischemic	0 (0)	23 (69)	19 (67)	<0.01	<0.01	0.06
H_2FPEF score (points)	0 (0)	4.5 (1–8)	…	…	…	…
Heart failure pharmacotherapy						
β Blocker	0 (0)	26 (81)	28 (100)	<0.01	<0.01	0.05
ARNI/ACEI/ARB	0 (0)	29 (87)	28 (100)	<0.01	<0.01	0.42
ARNI	0 (0)	2 (6.1)	16 (57)	0.71	<0.01	<0.01
ACEI	0 (0)	9 (27)	3 (11)	0.09	0.36	0.29
ARB	0 (0)	18 (55)	9 (32)	<0.01	0.02	0.13
Diuretics	0 (0)	24 (75)	28 (100)	<0.01	<0.01	0.01
Aldosterone antagonist	0 (0)	11 (34)	19 (68)	0.01	<0.01	0.02
Aspirin	0 (0)	11 (34)	7 (25)	0.03	0.07	0.61
Statins	0 (0)	24 (75)	21 (75)	<0.01	<0.01	1.00
Oral hypoglycemic agent	0 (0)	22 (69)	11 (39)	<0.01	<0.01	0.04
Insulin	0 (0)	6 (18)	6 (21)	0.17	0.17	1.00
Warfarin	0 (0)	10 (30)	3 (11)	0.05	0.36	0.18
Biomarkers						
High-sensitive troponin T, ng/dL	3 (3–6)	10 (7–16)	13 (7–19)	<0.01	<0.01	0.37
NT-proBNP, pg/mL	40 (19–50)	248 (79–574)	743 (250–2054)	<0.01	<0.01	<0.01
Laboratory testing						
Hemoglobin, mg/dL	14.27 (1.37)	13.63 (1.28)	13.69 (1.33)	0.28	0.28	0.86
Hematocrit, mg/dL	42.4 (4.5)	40.8 (3.5)	40.7 (3.4)	0.34	0.34	0.87
Creatinine, mg/dL	0.83 (0.15)	0.94 (0.30)	1.02 (0.35)	0.36	0.09	0.36

(*Continued*)

Table 1. Continued

Variables	Summary statistics			*P* values (Holm adj.)		
	Control N=20*	HFpEF N=33*	HFrEF N=28*	Control vs HFpEF	Control vs HFrEF	HFpEF vs HFrEF
Urea, mg/dL	32 (8)	41 (12)	41 (15)	0.06	0.06	0.93
Glucose, mg/dL	84 (4)	135 (77)	118 (48)	0.01	0.01	0.28
Serum potassium, mEq/L	4.30 (0.26)	4.50 (0.36)	4.38 (0.26)	0.10	0.38	0.32
Glycated hemoglobin, %	5.16 (0.3)	6.67 (1.3)	6.73 (2.4)	<0.01	<0.01	0.89
Total cholesterol, mg/dL	215 (41)	167 (43)	165 (47)	<0.01	<0.01	0.85
High-density lipoprotein cholesterol, mg/dL	59 (13)	41 (10)	40 (13)	<0.01	<0.01	0.86
Triglycerides, mg/dL	128 (113)	194 (138)	162 (97)	0.19	0.62	0.62
Resting ECG findings						
Atrial fibrillation	0 (0%)	6 (20%)	9 (32%)	0.45	0.39	0.45
LV hypertrophy (ECG)	0 (0%)	6 (20%)	9 (32%)	0.45	0.39	0.45
T inversion	6 (40%)	11 (33%)	8 (29%)	0.90	0.90	0.90
ST deviation	6 (40%)	5 (15%)	1 (3.6%)	0.19	0.02	0.28
QRS duration, ms	68 (18)	82 (20)	127 (50)	0.26	<0.01	<0.01
QT duration, ms	330 (54)	366 (46)	395 (72)	0.11	<0.01	0.11
Premature ventricular complex	0 (0)	1 (3.2)	0 (0)	1.00	1.00	1.00
Premature atrial complex	0 (0)	3 (9.1)	12 (43)	0.69	0.03	0.02
Left-bundle branch block	3 (25)	0 (0)	1 (3.6)	0.07	0.20	0.93
Right-bundle branch block	0 (0)	6 (20)	9 (32)	0.4	0.39	0.45

ACEI indicates angiotensin-converting enzyme inhibitor; ARB, angiotensin receptor blocker; ARNI, angiotensin receptor–neprilysin inhibitor; CABG, coronary artery bypass graft surgery; H_2FPEF, heavy, hypertensive, atrial fibrillation, pulmonary hypertension, elder, filling pressure; HFpEF, heart failure with preserved ejection fraction; HFrEF, heart failure with reduced ejection fraction; hs-cTnT, high-sensitivity cardiac troponin T; IQR, interquartile range; LV, left ventricular; NT-proBNP, N-terminal pro-B-type natriuretic peptide; NYHA, New York Heart Association; and PCI, percutaneous coronary intervention.

*n (%); median (IQR); mean (SD).

250–2054]; controls, 4 [IQR, 19–50] pg/mL; Table 1). Hs-cTnT (HFpEF, 10 [IQR, 7– 16]; HFrEF, 13 [IQR, 7–19]; controls, 3 [IQR, 3–6] ng/dL; Table 1), and glycated hemoglobin (HFpEF, 6.67±1.3; HFrEF, 6.73±2.4; controls, 5.16±0.3%; Table 1) were higher in patients with HF compared with controls (all *P*<0.01), fasting glucose levels (HFpEF, 135±77; HFrEF, 118±48; controls, 84±4 mg/dL; Table 1) were markedly increased in patients with HFpEF compared with controls (*P*=0.01). Patients with HF, regardless of phenotype, exhibited lower levels of total cholesterol compared with controls (HFpEF, 167±43; HFrEF, 165±47 mg/dL; controls, 215±41; controls versus HFpEF or HFrEF, *P*<0.01; Table 1). This observation is likely associated with the increased use of statins among patients with HF, with 75% (n=24) in the HFpEF group and 75% (n=21) in the HFrEF group.

^{123}Iodine-Meta-Iodobenzylguanidine

Cardiac sympathetic function was evaluated by myocardial scintigraphy with ^{123}I-MIBG, which revealed significant differences between study groups in terms of both the delayed (4 hours) H/M ratio and washout rate (Table 2 and Figure 2A). The delayed H/M ratio was significantly lower in patients with HF, especially among HFrEF, when compared with HFpEF or controls (HFpEF, 1.59±0.25; HFrEF, 1.45±0.16; controls, 1.92±0.24; all comparison *P*<0.01; Figure 2A, Table 2).

Table 2. Myocardial Scintigraphy With ^{123}I-MIBG of Study Participants

Variables	Summary statistics			*P* values (Holm adj.)		
	Control, N=20*	HFpEF, N=33*	HFrEF, N=28*	Control vs HFpEF	Control vs HFrEF	HFpEF vs HFrEF
Early H/M ratio (15 min)	1.78 (0.16)	1.63 (0.20)	1.58 (0.12)	<0.01	<0.01	0.26
Delayed H/M ratio (4 h)	1.92 (0.24)	1.59 (0.25)	1.45 (0.16)	<0.01	<0.01	0.01
Washout rate	3 (29)	30 (18)	36 (14)	<0.01	<0.01	0.22

HFpEF indicates heart failure with preserved ejection fraction; HFrEF, heart failure, and H/M, heart-to-mediastinum.

*n (%); median (IQR); mean (SD).

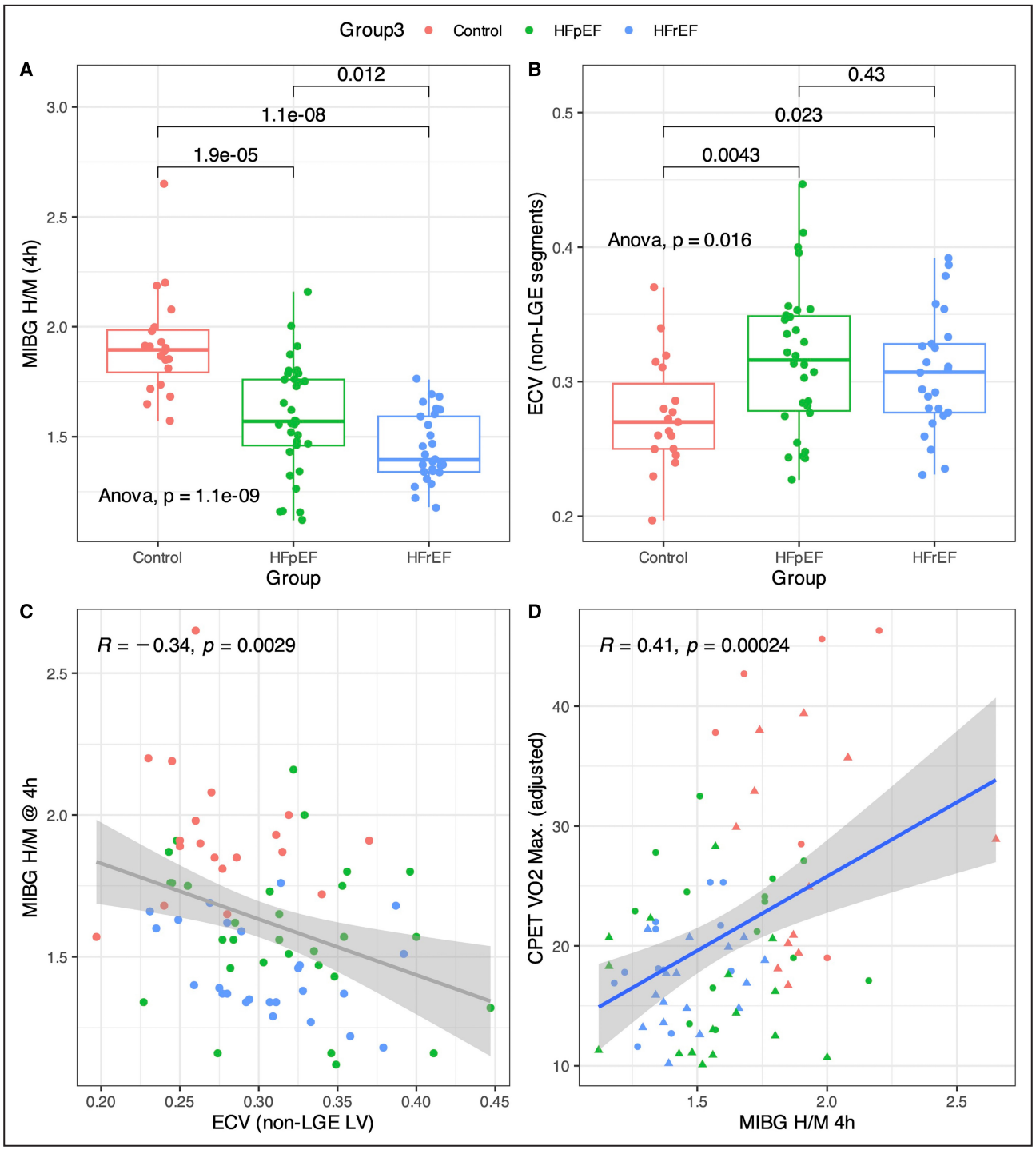

Figure 2. **^{123}I-MIBG H/M, CMR-ECV, and CPET results across study groups.**
A, ^{123}I-MIBG H/M at 4 h was significantly diminished in HFrEF and HFpEF compared with healthy controls, with HFrEF showing a more pronounced reduction in sympathetic function than HFpEF. **B**, The extracellular volume (ECV) fraction, a marker of diffuse interstitial fibrosis was significantly higher in HF patients compared with healthy controls, but there was no significant ECV difference between patients with HF with and without reduced ejection fraction. **C**, The myocardial ECV correlated inversely with ^{123}I-MIBG H/M at 4 h (Spearman r=−0.34, P=0.0029), suggesting that ECV expansion reduces sympathetic innervation density, leading to a reduced ^{123}I-MIBG H/M. **D**, The adjusted peak Vo_2 was inversely correlated with ^{123}I-MIBG H/M at 4 h. CMR indicates cardiac magnetic resonance; CPET, cardiopulmonary exercise capacity; HF, heart failure; HFpEF, heart failure with preserved ejection fraction; HFrEF, heart failure with reduced ejection fraction; H/M, heart-to-mediastinum; ^{123}I-MIBG, ^{123}iodine-meta-iodobenzylguanidine; Vo_2, oxygen consumption.

The washout rate was higher among patients with HF (HFpEF, 30±18; HFrEF, 36±14; controls, 3±29; controls versus HFpEF or HFrEF, $P<0.01$; Table 2).

Echocardiography

The parameters obtained through echocardiographic examination are summarized in Table S1. As expected, patients with HFrEF had a significantly reduced LVEF compared with both patients with HFpEF and controls (HFpEF, 59±8%; HFrEF, 33±9%; controls, 65±7%; all comparisons, $P<0.01$; Table S1).

Furthermore, patients with HFrEF and those with HFpEF manifested distinct patterns of LV remodeling. Patients with HFpEF exhibited significantly smaller LV mass and volumes in comparison with patients with HFrEF (Table S1). Additionally, end-diastolic relative wall thickness was larger in HFpEF patients compared with HFrEF (HFpEF, 0.34±0.04 versus HFrEF, 0.27±0.07; $P<0.01$; Table S1) and the indexed diastolic and systolic LV volumes were smaller in HFpEF versus HFrEF (Table S1). Finally, global longitudinal strain (GLS) was markedly reduced in both HF groups compared with controls and, as expected, more so in HFrEF compared with HFpEF (HFpEF, –16.2±4%; HFrEF, –8.1±3.6%; controls, –19.5±2.9%; all comparisons, $P<0.01$).

CMR Imaging Assessment

Parameters obtained through CMR are shown in Table 3. Patients with HFrEF had a significantly reduced LVEF compared with both patients with HFpEF and controls (HFrEF, 30±9%; HFpEF, 60±10%; controls, 65±5%). Patients with HF had a higher LV mass index. The LV cardiomyocyte mass, calculated as LV mass index*(1–ECV), was higher in both HF phenotypes compared with the control group (HFrEF, 53 [IQR, 42–78]; HFpEF, 41 [IQR, 31–48]; controls, 32 [IQR, 28–37] g/m^2; all comparisons, $P\leq0.02$; Table 3). The right ventricular mass index was similar in all subgroups, but right ventricular ejection fraction was significantly lower in patients with HFrEF compared with controls (Table 3). Patients with HF, regardless of phenotype, had an expanded ECV compared with controls, indicating a higher burden of interstitial fibrosis and adverse tissue remodeling, and ECV was similar between the HF subgroups (ECV, HFpEF 0.32±0.05%

Table 3. CMR Characteristics of Study Participants

Variables	Summary statistics			*P* values (Holm adj.)		
	Control, N=20*	HFpEF, N=33*	HFrEF, N=28*	Control vs HFpEF	Control vs HFrEF	HFpEF vs HFrEF
LV mass index, g/m^2	44 (8)	62 (22)	87 (44)	0.05	<0.01	<0.01
LVEDV index, mL/m^2	68 (11)	73 (29)	151 (81)	0.75	<0.01	<0.01
LVESV index, mL/m^2	24 (5)	30 (19)	112 (74)	0.61	<0.01	<0.01
LVSV index, mL/m^2	44 (8)	42 (4)	40 (9)	0.58	0.18	0.57
LVEF, %	65 (5)	60 (10)	30 (9)	0.03	<0.01	<0.01
LAVI, mL/m^2	25 (8)	36 (17)	39 (20)	0.06	0.02	0.48
LV/RV mass ratio	0.67 (0.12)	0.93 (0.34)	0.60 (0.16)	<0.01	0.36	<0.01
RV mass index, g/m^2	15 (4)	14 (5)	17 (4)	0.15	0.10	0.12
RVEDV index, mL/m^2	70 (11)	60 (2)	68 (25)	<0.01	0.29	0.18
RVESV index, mL/m^2	33 (5)	30 (1)	38 (20)	0.07	0.34	0.08
RVSV index, mL/m^2	40 (6)	30 (9)	30 (8)	0.01	0.50	0.08
RVEF, %	53 (2)	49 (9)	45 (10)	0.03	<0.01	0.14
Native T2, ms	53 (9)	56 (8)	58 (9)	0.58	0.32	0.58
Native T1, ms	1210 (84)	1259 (67)	1269 (71)	0.05	0.03	0.62
ECV, %	0.276 (0.04)	0.319 (0.06)	0.309 (0.05)	0.01	0.06	0.48
ECV (no LGE), %	0.276 (0.04)	0.317 (0.05)	0.306 (0.04)	<0.01	0.02	0.43
LV cardiomyocyte mass, g/m^2 (IQR)	32 (28, 37)	41 (31, 48)	53 (42, 78)	0.02	<0.01	0.01
Presence of LGE	0 (0)	16 (50)	19 (70)	<0.01	<0.01	0.19
LGE typical for coronary artery disease	0 (0, 0)	4 (11.8)	1 (3.6)	<0.01	<0.01	0.27
LGE mass, g/m^2	0	10.5 (6, 16)	10.7 (6, 21)	<0.01	<0.01	0.91

ECV indicates extracellular volume; HFpEF, heart failure with preserved ejection fraction; HFrEF, heart failure with reduced ejection fraction; IQR, interquartile range; LAVI, left atrial volume index; LGE, late gadolinium enhancement; LV, left ventricular; LVEDV, left ventricular end-diastolic volume; LVEF, left ventricular ejection fraction; LVESV, left ventricular end-systolic volume; LVSV, left ventricular stroke volume; RV, right ventricular; RVEDV, right ventricular end-diastolic volume; RVEF, right ventricular ejection fraction; RVESV, right ventricular end-systolic volume; RVSV, right ventricular stroke volume.

*n (%); median (IQR); mean (SD).

versus HFrEF 0.31±0.04; *P*=0.43; Figure 2B, Table 3; native T1, HFpEF, 1259±67 versus HFrEF, 1269±71 ms; *P*=0.62). ECV did not exhibit a significant correlation with systolic performance in both HFpEF and HFrEF, but correlated with the diastolic function indexes, E/A (*R*=0.45, *P*=0.03) and E/e′ (*R*=0.43, *P*=0.03) among HFrEF (Figure S1C and S1D).

Cardiopulmonary Exercise Testing

Assessment of cardiopulmonary exercise capacity, measured by maximum oxygen uptake during exercise (peak V_{O_2}; Table S2), indicated that all patients with HF had a considerable degree of exercise limitation, which was more noticeable in the HFrEF group (HFpEF, 19±6; HFrEF, 18±4; controls, 30±10 mL/min per kg, Table S2). The exercise capacity, assessed through the adjusted peak V_{O_2}, exhibited a notable association with the delayed H/M ratio ^{123}I-MIBG H/M (*R*=0.41, *P*<0.01, Figure 2D) and ECV (*R*=−0.34, *P*<0.01; Figure 2C).

Cardiac Sympathetic Activity in HFpEF and HFrEF

Both HFrEF and HFpEF patients had a decreased early H/M ratio (HFpEF, 1.63±0.20; HFrEF, 1.58±0.12; controls; 1.78±0.16; Table 2) and H/M ratio (HFpEF, 1.59±0.25; HFrEF, 1.45±0.16; controls, 1.92±0.24; all comparison, *P*<0.01; Figure 2A, Table 2). The washout rate was abnormally high in both HFpEF and HFrEF groups (HFpEF, 30±18; HFrEF, 36±14; controls, 3±29; controls versus HFpEF or HFrEF, *P*<0.01; Table 2).

Cardiac Sympathetic Function, Myocardial Remodeling, and Biomarkers (NT-proBNP and hs-cTnT)

In patients with HFrEF, LVEF exhibited a significant correlation (*R*=0.41, *P*<0.04) with ^{123}I-MIBG H/M ratio, whereas no such correlation was observed in patients with HFpEF (Figure S1A). Furthermore, within the cohort of patients with HFrEF, there was an observed trend correlation between the diastolic function index E/e′ and the ^{123}I-MIBG H/M ratio (*R*=−0.34, *P*=0.08).

Patients with HF showed an inverse association between delayed H/M ratio and makers of unfavorable myocardial remodeling as assessed through echocardiogram and CMR, indicating that the greater the cardiac remodeling, the lower the uptake of ^{123}I-MIBG by sympathetic receptors. Figure S2 presents an overview of the correlations between ^{123}I-MIBG data and several imaging variables of interest for all study participants. Study participants with reduced GLS generally had a lower delayed ^{123}I-MIBG H/M ratio (*R*=−0.54, *P*<0.01; Figure S2). Notably, the inverse correlation between GLS and the delayed H/M ratio, when assessed independently for each HF phenotype, was only significant in HFrEF and not in HFpEF (HFrEF, *R*=−0.53, *P*=0.0037; HFpEF, *R*=−0.036, *P*=0.85; Figure S1). Similarly, elevated interstitial fibrosis assessed by "remote" ECV (ie, ECV average with exclusion of segments with LGE) was associated with a lower late H/M (*R*=−0.34, *P*<0.01; Figure 2C and Figure S2). Additionally, NT-proBNP, an important diagnostic and prognostic marker for HF, showed a negative correlation with delayed H/M (R= −0.59, *P*<0.01; Figure S2).

Hs-cTnT levels were elevated in patients with HF compared with controls (HF, 10.5 [IQR, 6.8–18.1]; controls, 3.2 [IQR, 3.0–6.1]; *P*<0.001). Within the HF group, patients with HFrEF had only nominally higher hs-cTnT (HFpEF, 10.3 [IQR, 6.6–15.8]; HFrEF, 13.5 [IQR, 7.2–19.1]; *P*=0.4). Hs-cTnT exhibited significant correlations with various imaging variables of interest, including late H/M ^{123}I-MIBG (R=−0.5, *P*<0.01), ^{123}I-MIBG washout (R=0.35, *P*<0.01), GLS (*R*=0.57, *P*<0.01), E/e′ (*R*=0.51, *P*<0.01), ECV remote (*R*=0.23, *P*<0.01), LV mass index (*R*=0.51, *P*<0.05), LV end-diastolic volume index (*R*=0.4, *P*<0.05), LVEF (*R*=−0.48, *P*<0.01), LV mass/end-diastolic volume (*R*=0.21, *P*<0.01), and native T2 (*R*=0.32, *P*<0.01), as shown in Figure S2.

Mediation Analysis

A mediation model illustrated by the path diagram in Figure S3 was built to investigate to what degree ^{123}I-MIBG H/M mediated the effect of ECV on NT-proBNP. The analysis with this model suggested the absence of a direct effect of ECV on NT-proBNP (direct effect of ECV, 4.93±5.14; *P*=0.34), and a significant mediation effect by ^{123}I-MIBG H/M (indirect effect, 9.49±3.41; *P*<0.01, root mean square error of approximation <0.01). This mediation effect of the delayed H/M ratio suggests that ECV expansion contributes to a reduced sympathetic innervation density, with ECV expansion evident in HF compared with control subjects (Figure S3).

DISCUSSION

The present study of patients with HF with preserved and reduced ejection fraction shows for the first time how cardiac sympathetic function is associated with myocardial extracellular matrix expansion assessed by CMR-based measurements of the ECV. "Sympathetic function" assessed by ^{123}I-MIBG single-photon emission computed tomography encompasses the effects of several factors relevant to functional and anatomic denervation in HF, such as sympathetic nerve density, neuronal integrity, sympathetic nerve activity, and sympathetic tone.[19] Autonomic innervation density is adversely affected by myocardial interstitial fibrosis. ECV determined by CMR T1-mapping is a well-established imaging biomarker of interstitial fibrosis.

The observation in this study of a negative correlation between ECV expansion and sympathetic function suggests that nerve density plays a prominent role in the impairment of sympathetic function in HF and this manifests by a decrease of the H/M ratio on delayed ^{123}I-MIBG images. Furthermore, in our investigation, the delayed H/M from ^{123}I-MIBG exhibited notable correlations with several indicators of ventricular remodeling and dysfunction, including LV end-diastolic volume index, LV mass index, and LV cardiomyocyte mass index, global longitudinal strain and diastolic function (E/e′ from echocardiography) as shown in Figure S3. Additionally, the delayed H/M ratio correlated with NT-proBNP and hs-cTnT, both of which are powerful predictors of cardiovascular death. The signs of the correlations suggest that compromised cardiac sympathetic dysfunction, manifested by a reduced H/M ratio, is linked to LV hypertrophy, diastolic dysfunction, reduced ventricular strain, and myocardial damage assessed by an hs-cTnT test.

Activation of the sympathetic nervous system has long been recognized as a distinct characteristic of the clinical syndrome of HF(21), which would entail higher sympathetic nerve activity, while ECV expansion, commonly seen in HF, would reduce innervation density. Sympathetic nervous system hyperactivity is an initial compensatory mechanism in HF to stimulate contractility and maintain cardiac output but ultimately leads to lower β-adrenergic receptor responsiveness and density. This desensitization of myocardial β-adrenergic receptors can reflect an impairment of the norepinephrine neuronal uptake function, which can be evaluated by ^{123}I-MIBG, and also an increase in circulating norepinephrine concentrations. In this study, cardiac sympathetic function was most impaired in HFrEF, and in this subgroup, there was a significant correlation between sympathetic function and systolic performance assessed by LVEF and GLS (Figure S1). Sympathetic function was lower in HFpEF compared with controls (Figure 1A), without a significant association with systolic and diastolic performance, suggesting that β-adrenergic receptor responsiveness and sympathetic function are partially preserved in the early stages of HF or when LVEF is preserved or marginally depressed.[20] The mediation analysis provided (Figure S2) does not suggest that autonomic dysfunction, as assessed by the ^{123}I-MIBG H/M ratio, is the exclusive mediator in the impact of ECV or NT-proBNP on HF severity. Instead, our aim was to highlight that autonomic dysfunction plays a mediating role, acknowledging the potential involvement of other mediators as well.

Previous studies have shown that there is a strong correlation between cardiac scintigraphy with ^{123}I-MIBG and norepinephrine levels, given that ^{123}I-MIBG is a norepinephrine analog that emerges as an important tool to detect abnormalities of the adrenergic system in patients with HF. Norepinephrine is an important mediator in the sympathetic nerve system, and multiple studies demonstrated that high plasma norepinephrine concentration is associated with a decrease of ^{123}I-MIBG uptake in HF, and this phenomenon has been explained as sympathetic denervation. Also, ^{123}I-MIBG was proven to have a high prognostic power in HFrEF, but more studies are required to clarify its value in predicting adverse events in HFpEF.[7,21]

Previous studies have established a strong link between abnormal myocardial sympathetic innervation and prognosis. Shah and colleagues[22] conducted a study to investigate the potential correlation between LVEF and myocardial innervation assessed with ^{123}I-MIBG, as well as its impact on outcomes among patients with HF included in the ADMIRE-HF (AdreView Myocardial Imaging for Risk Evaluation in Heart Failure) study.[6] In this study, the ^{123}I-MIBG (H/M) ratio of <1.6 identified patients with HF at high risk of major cardiovascular events (death or arrhythmic event), independent of whether LVEF is ≤35% (adjusted hazard ratio, 2.39 [95% CI, 1.03–5.55] versus 5.28 [95% CI, 1.21–23.02]; interaction of LVEF with H/M, P=0.48). However, it is important to note that this analysis did not explore the relationship between myocardial sympathetic innervation and available data on myocardial remodeling. Moreover, the study relied solely on LVEF, which provides a suboptimal characterization of myocardial remodeling and did not include data from contemporary noninvasive imaging techniques such as myocardial strain assessed by echocardiography or T1 mapping data obtained through CMR imaging. In our investigation, we identified a significant correlation between cardiac sympathetic function and indicators of functional capacity, as demonstrated by adjusted peak Vo_2 max (Figure 1D). Additionally, we detected a significant link between sympathetic innervation and interstitial fibrosis, as assessed using CMR ECV (Figure 1C). Of particular interest is the observation that sympathetic innervation appears to exert a constraining influence on a global longitudinal strain by echocardiography in HFrEF (Figure S1B). Nevertheless, our data suggest that in HFpEF, longitudinal strain remains largely uninfluenced by sympathetic function.

To date, only a small number of studies correlated CMR tissue markers with ^{123}I-MIBG scintigraphy. Barizon et al[23] demonstrated in a small cohort of patients with Chagas disease that the spatial distribution of fibrosis and of perfusion defects in the heart coincided with sympathetic dysfunction. We observed abnormally increased ECV, a marker of interstitial fibrosis, in both patients with HFrEF and patients with HFpEF, and found it to be associated with reduced cardiac sympathetic function. Furthermore, Verschure et al[24] suggested that inflammation and cardiac sympathetic

activity are not related in patients with stable CHF. Inflammation is a key regulator of the reparative response leading to myocardial fibrosis and myocardial fibrosis may represent a cumulative effect, resulting in lower innervation density and a correlation of sympathetic function and ECV. In a separate investigation by Cruz et al, GLS and delayed H/M correlated with strength, which is consistent with the results of our study.[25]

LIMITATIONS

Several significant limitations should be taken into account when interpreting the findings of this study. First, this study was conducted at a single center, involving a relatively limited number of patients from a tertiary HF clinic. Therefore, caution should be exercised when generalizing the results to other HF cohorts. Second, despite achieving reasonable matching in terms of including a comparable proportion of women in all participant groups, attaining similar age profiles was not possible. Third, the imaging techniques employed in this study are not routinely recommended and performed in all patients with HF. This study lacks data from stress echocardiography and invasive hemodynamic measurements, both of which could provide valuable additional insights. The selected LVEF threshold of 45% for delineating HFrEF and HFpEF at the inception of this study predates the more recent publication of several seminal contemporary HF studies suggesting refinements in these definitions. There is also considerable overlap of the imaging biomarkers ECV and ^{123}I-MIBG H/M among the different groups. Although the HF cohort was medically well-managed population according to available HF guidelines, certain novel HF medications, particularly sodium–glucose transport protein 2 inhibitors, had not yet been formally incorporated into the prevailing guidelines, and individuals with HF recruited for this study were not receiving this specific treatment at that time. Finally, while our findings are novel and could provide valuable insights into HF pathophysiology, it is important to recognize that the limited sample size of the current study provides mostly hypothesis-generating insights that require wider clinical validation in a larger and more diverse patient cohort.

CONCLUSIONS

Cardiac sympathetic function assessed by the delayed H/M ratio from ^{123}I-MIBG images was abnormal in patients with HF with reduced and preserved ejection fraction as compared with controls. Cardiac sympathetic dysfunction correlated with extracellular matrix expansion, suggesting that this form of adverse tissue remodeling may reduce sympathetic innervation density. Cardiac sympathetic dysfunction appears to be more of a limiting factor in HFrEF than HFpEF for LVEF and GLS. This is consistent with the notion that HFrEF is characterized by β-adrenergic receptor desensitization and reduced receptor density contributing to systolic dysfunction compared with HFpEF.

ARTICLE INFORMATION

Received February 29, 2024; accepted May 31, 2024.

Affiliations

Faculdade de Ciências Médicas, Universidade Estadual de Campinas, São Paulo, Brazil (L.M.d.S., A.C., L.R.P., A.A.B., C.N.G., S.P., V.C.R., W.E.M.R., J.R.M., R.S., L.A., A.S., W.N., C.D.R., O.R.C.); Cardiovascular Imaging Research Center, Division of Cardiology and Department of Radiology, Massachusetts General Hospital, Harvard Medical School, Boston, MA (T.N.); and Non-Invasive Cardiovascular Imaging Program, Department of Radiology, Brigham and Women's Hospital and Harvard Medical School, Boston, MA (M.J.).

Sources of Funding

Dr. Coelho-Filho is supported by grant in research productivity (303366/2015-0) from the National Council for Scientific and Technological Development and by grants from the São Paulo State Research Foundation (2015/15402-2, 2016/26209-1 and 2017/03708-5). Dr. Jerosch-Herold was supported by R01AG052282 from the National Institutes of Health.

Disclosures

Dr. Coelho-Filho reports receiving research grants and speaking honoraria from AstraZeneca, Bayer, Novartis, and Pfizer. The remaining authors have no disclosures to report.

Supplemental Material

Tables S1–S2
Figures S1–S3

REFERENCES

1. Abouezzeddine OF, Redfield MM. Who has advanced heart failure?: definition and epidemiology. *Congest Heart Fail*. 2011;17:160–168. doi: 10.1111/j.1751-7133.2011.00246.x
2. Guha K, McDonagh T. Heart failure epidemiology: European perspective. *Curr Cardiol Rev*. 2013;9:123–127. doi: 10.2174/1573403x11309020005
3. Truby LK, Rogers JG. Advanced heart failure: epidemiology, diagnosis, and therapeutic approaches. *JACC Heart Fail*. 2020;8:523–536. doi: 10.1016/j.jchf.2020.01.014
4. Heidenreich PA, Bozkurt B, Aguilar D, Allen LA, Byun JJ, Colvin MM, Deswal A, Drazner MH, Dunlay SM, Evers LR, et al. 2022 AHA/ACC/HFSA Guideline for the Management of Heart Failure: a report of the American College of Cardiology/American Heart Association Joint Committee on Clinical Practice Guidelines. *Circulation*. 2022;145:e895–e1032. doi: 10.1161/CIR.0000000000001063
5. McDonagh TA, Metra M, Adamo M, Gardner RS, Baumbach A, Bohm M, Burri H, Butler J, Celutkiene J, Chioncel O, et al. 2023 Focused Update of the 2021 ESC Guidelines for the diagnosis and treatment of acute and chronic heart failure. *Eur Heart J*. 2023;44:3627–3639. doi: 10.1093/eurheartj/ehad195
6. Jacobson AF, Senior R, Cerqueira MD, Wong ND, Thomas GS, Lopez VA, Agostini D, Weiland F, Chandna H, Narula J, et al. Myocardial iodine-123 meta-iodobenzylguanidine imaging and cardiac events in heart failure. Results of the prospective ADMIRE-HF (AdreView Myocardial Imaging for Risk Evaluation in Heart Failure) study. *J Am Coll Cardiol*. 2010;55:2212–2221. doi: 10.1016/j.jacc.2010.01.014
7. Katoh S, Shishido T, Kutsuzawa D, Arimoto T, Netsu S, Funayama A, Ishino M, Niizeki T, Nishiyama S, Takahashi H, et al. Iodine-123-metaiodobenzylguanidine imaging can predict future cardiac events in heart failure patients with preserved ejection fraction. *Ann Nucl Med*. 2010;24:679–686. doi: 10.1007/s12149-010-0409-3

8. Treibel TA, Fridman Y, Bering P, Sayeed A, Maanja M, Frojdh F, Niklasson L, Olausson E, Wong TC, Kellman P, et al. Extracellular volume associates with outcomes more strongly than native or post-contrast myocardial T1. *JACC Cardiovasc Imaging*. 2020;13:44–54. doi: 10.1016/j.jcmg.2019.03.017
9. McKee PA, Castelli WP, McNamara PM, Kannel WB. The natural history of congestive heart failure: the Framingham study. *N Engl J Med*. 1971;285:1441–1446. doi: 10.1056/NEJM197112232852601
10. Bozkurt B, Coats AJ, Tsutsui H, Abdelhamid M, Adamopoulos S, Albert N, Anker SD, Atherton J, Bohm M, Butler J, et al. Universal definition and classification of heart failure: a report of the Heart Failure Society of America, Heart Failure Association of the European Society of Cardiology, Japanese Heart Failure Society and Writing Committee of the Universal Definition of Heart Failure. *J Card Fail*. 2021;27(4):387–413. doi: 10.1016/j.cardfail.2021.01.022
11. Reddy YNV, Carter RE, Obokata M, Redfield MM, Borlaug BA. A simple, evidence-based approach to help guide diagnosis of heart failure with preserved ejection fraction. *Circulation*. 2018;138:861–870. doi: 10.1161/CIRCULATIONAHA.118.034646
12. Lang RM, Badano LP, Mor-Avi V, Afilalo J, Armstrong A, Ernande L, Flachskampf FA, Foster E, Goldstein SA, Kuznetsova T, et al. Recommendations for cardiac chamber quantification by echocardiography in adults: an update from the American Society of Echocardiography and the European Association of Cardiovascular Imaging. *J Am Soc Echocardiogr*. 2015;28:1–39.e14. doi: 10.1016/j.echo.2014.10.003
13. Flotats A, Carrió I, Agostini D, Le Guludec D, Marcassa C, Schäfers M, Schaffers M, Somsen GA, Unlu M, Verberne HJ, et al. Proposal for standardization of 123I-metaiodobenzylguanidine (MIBG) cardiac sympathetic imaging by the EANM Cardiovascular Committee and the European Council of Nuclear Cardiology. *Eur J Nucl Med Mol Imaging*. 2010;37:1802–1812. doi: 10.1007/s00259-010-1491-4
14. Spieker M, Katsianos E, Gastl M, Behm P, Horn P, Jacoby C, Schnackenburg B, Reinecke P, Kelm M, Westenfeld R, et al. T2 mapping cardiovascular magnetic resonance identifies the presence of myocardial inflammation in patients with dilated cardiomyopathy as compared to endomyocardial biopsy. *Eur Heart J Cardiovasc Imaging*. 2018;19:574–582. doi: 10.1093/ehjci/jex230
15. Coelho-Filho OR, Shah RV, Mitchell R, Neilan TG, Moreno H Jr, Simonson B, Kwong R, Rosenzweig A, Das S, Jerosch-Herold M. Quantification of cardiomyocyte hypertrophy by cardiac magnetic resonance: implications for early cardiac remodeling. *Circulation*. 2013;128:1225–1233. doi: 10.1161/CIRCULATIONAHA.112.000438
16. Neilan TG, Coelho-Filho OR, Shah RV, Abbasi SA, Heydari B, Watanabe E, Chen Y, Mandry D, Pierre-Mongeon F, Blankstein R, et al. Myocardial extracellular volume fraction from T1 measurements in healthy volunteers and mice: relationship to aging and cardiac dimensions. *JACC Cardiovasc Imaging*. 2013;6:672–683. doi: 10.1016/j.jcmg.2012.09.020
17. Coelho-Filho OR, Mongeon FP, Mitchell R, Moreno H Jr, Nadruz W Jr, Kwong R, Jerosch-Herold M. Role of transcytolemmal water-exchange in magnetic resonance measurements of diffuse myocardial fibrosis in hypertensive heart disease. *Circ Cardiovasc Imaging*. 2013;6:134–141. doi: 10.1161/CIRCIMAGING.112.979815
18. Lewis GD, Shah R, Shahzad K, Camuso JM, Pappagianopoulos PP, Hung J, Tawakol A, Gerszten RE, Systrom DM, Bloch KD, et al. Sildenafil improves exercise capacity and quality of life in patients with systolic heart failure and secondary pulmonary hypertension. *Circulation*. 2007;116:1555–1562. doi: 10.1161/CIRCULATIONAHA.107.716373
19. Zelt JGE, deKemp RA, Rotstein BH, Nair GM, Narula J, Ahmadi A, Beanlands RS, Mielniczuk LM. Nuclear imaging of the cardiac sympathetic nervous system: a disease-specific interpretation in heart failure. *JACC Cardiovasc Imaging*. 2020;13:1036–1054. doi: 10.1016/j.jcmg.2019.01.042
20. Seo M, Yamada T, Tamaki S, Watanabe T, Morita T, Furukawa Y, Kawasaki M, Kikuchi A, Kawai T, Nakamura J, et al. Prognostic significance of cardiac (123)I-MIBG SPECT imaging in heart failure patients with preserved ejection fraction. *JACC Cardiovasc Imaging*. 2022;15:655–668. doi: 10.1016/j.jcmg.2021.08.003
21. Jacobson AF, Lombard J, Banerjee G, Camici PG. 123I-mIBG scintigraphy to predict risk for adverse cardiac outcomes in heart failure patients: design of two prospective multicenter international trials. *J Nucl Cardiol*. 2009;16:113–121. doi: 10.1007/s12350-008-9008-2
22. Shah AM, Bourgoun M, Narula J, Jacobson AF, Solomon SD. Influence of ejection fraction on the prognostic value of sympathetic innervation imaging with iodine-123 MIBG in heart failure. *JACC Cardiovasc Imaging*. 2012;5:1139–1146. doi: 10.1016/j.jcmg.2012.02.019
23. Barizon GC, Simões MV, Schmidt A, Gadioli LP, Murta Junior LO. Relationship between microvascular changes, autonomic denervation, and myocardial fibrosis in Chagas cardiomyopathy: evaluation by MRI and SPECT imaging. *J Nucl Cardiol*. 2020;27:434–444. doi: 10.1007/s12350-018-1290-z
24. Verschure DO, Lutter R, van Eck-Smit BLF, Somsen GA, Verberne HJ. Myocardial (123)I-mIBG scintigraphy in relation to markers of inflammation and long-term clinical outcome in patients with stable chronic heart failure. *J Nucl Cardiol*. 2018;25:845–853. doi: 10.1007/s12350-016-0697-7
25. Cruz MC, Abreu A, Portugal G, Santa-Clara H, Cunha PS, Oliveira MM, Santos V, Oliveira L, Rio P, Rodrigues I, et al. Relationship of left ventricular global longitudinal strain with cardiac autonomic denervation as assessed by. *J Nucl Cardiol*. 2019;26:869–879. doi: 10.1007/s12350-017-1148-9